Thermal convection with evolving surface in a rotating icy satellite

Miroslav Kuchta
Geodynamický seminár KG

April 18, 2012

Albedo Dichotomy

- leading dark side - albedo 0.04
- trailing bright side - albedo 0.6
- exogenous origin - volcanism
- endogenous origin - deposits

Flattening

- $747.4 \pm 3.1 \times 712.3 \pm 2$ km consistent with $T_{rot} \approx 16\,h$
- observed $T_{rot} = 79.33\,d$
- frozen shape: Robuchon et al. [2010], Castillo-Rogez et al. [2007]

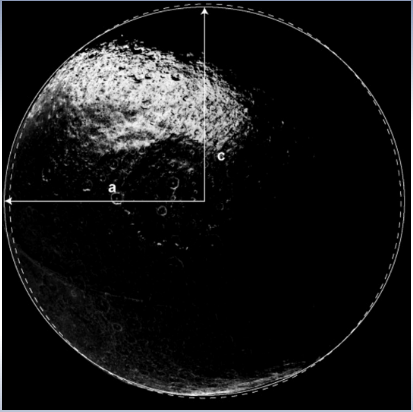

Equatorial Ridge

- endogenous origin: Ip [2006], Levison et al. [2011]
- origin due to contraction: Sandwell and Schubert [2010]
- origin related to convection: Czechowski and Leliwa-Kopystynski [2008]

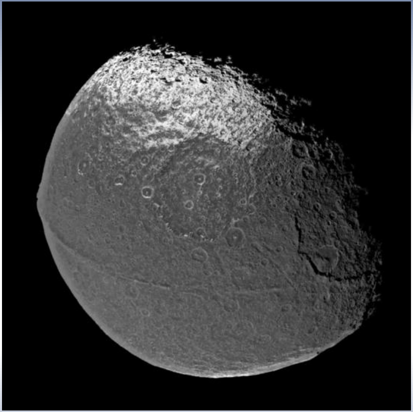

Equatorial Ridge

- endogenous origin: Ip [2006], Levison et al. [2011]
- origin due to contraction: Sandwell and Schubert [2010]
- origin related to convection: Czechowski and Leliwa-Kopystynski [2008]

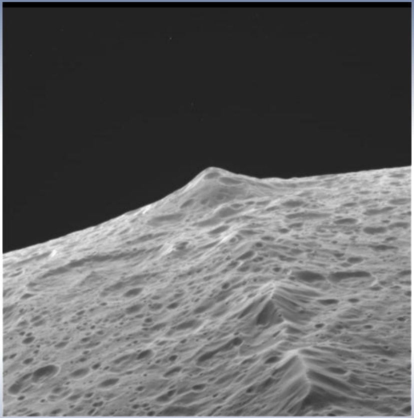

Governing Equations

$$\left.\begin{aligned} \nabla \cdot \vec{v} &= 0 \\ -\rho \frac{\mathrm{D}\vec{v}}{\mathrm{D}t} - \nabla \pi + \nabla \cdot \left(\eta \left(\nabla \vec{v} + (\nabla \vec{v})^{\mathsf{T}}\right)\right) + \rho \vec{f} &= 0 \\ \rho_0 c_p \left(\frac{\partial T}{\partial t} + \vec{v} \cdot \nabla T\right) &= \nabla \cdot (k \nabla T) + q + \boldsymbol{\sigma} : \nabla \vec{v} \end{aligned}\right\} \qquad \Omega_t \times (0, T]$$

$$\rho = \rho_0(1 - \alpha(T - T_0)),\ \alpha = \mathit{const} > 0$$

$$\eta = \eta(T, \dot{\epsilon}_{II}, d)$$

$$k = \mathit{const} > 0,\ c_p = \mathit{const} > 0$$

$$\vec{f} = \vec{g}(|\vec{x}|) + \vec{b}(\vec{x})$$

Boundary Conditions

- $(\Gamma_1 \cup \Gamma_2) \times [0, T]$: symmetry
- $\Gamma_3 \times [0, T]$: no-slip, zero heat flux
- $\Gamma_t \times [0, T]$: free-surface, prescribed temperature

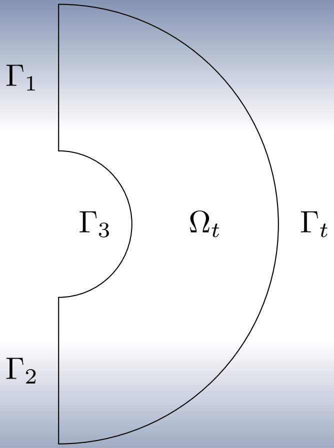

Variable Density Approximation

- $\Omega \supset \Omega_t,\ \partial\Omega = \Gamma_1 \cup \Gamma_2 \cup \Gamma_3 \cup \Gamma_4$
- $\Gamma_4 \times [0, T]$: free-slip, prescribed temperature
- ice $:= \{\vec{x} \,|\, \vec{x} \in \Omega_t\}$
  air $:= \{\vec{x} \,|\, \vec{x} \in (\Omega - \Omega_t)\}$
- $\rho_{0,\text{air}} \ll \rho_{0,\text{ice}},\ \eta_{0,\text{air}} \ll \eta_{0,\text{ice}}$

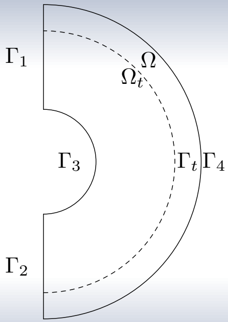

Surface Tracking

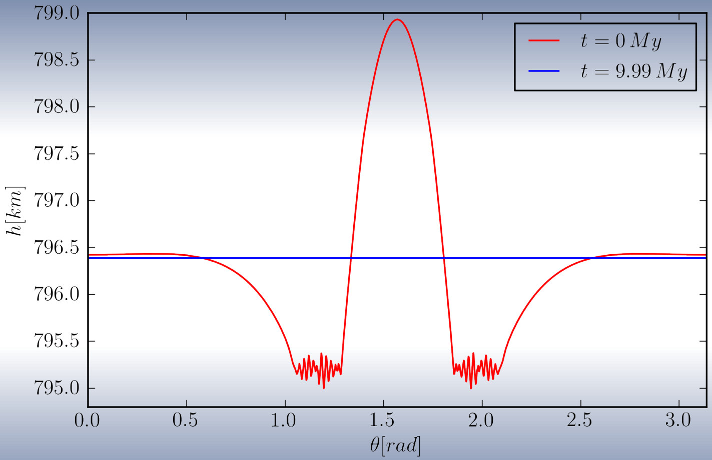

Surface Tracking

- material surface $H(r, \theta, t) = 0$
- evolution $\frac{\partial H}{\partial t} + \vec{v} \cdot \nabla H + \epsilon \Delta H = 0$
- “nice” surface deformations allow $r = h(\theta, t)$
- symmetry BC on poles

Implementation

- Stokes problem: solved in Ω, FD on staggered grid
- Balance of energy: solved in Ω_t, FD, semi-implicit with upwinding
- Advection of surface: FD, semi-implicit with upwinding, linear interpolation of ρ near surface

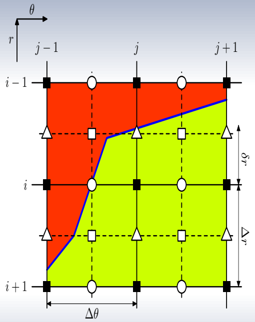

Radiogenic Heating Without Centrifugal Force

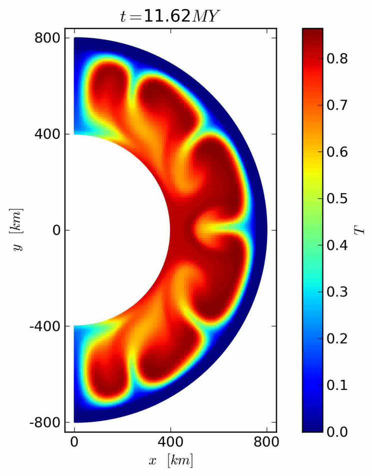

Radiogenic Heating With Centrifugal Force

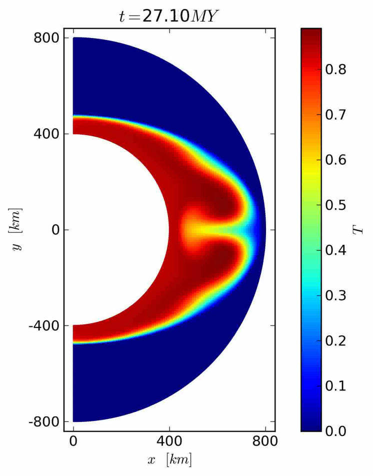

Manual Exponential Despinning

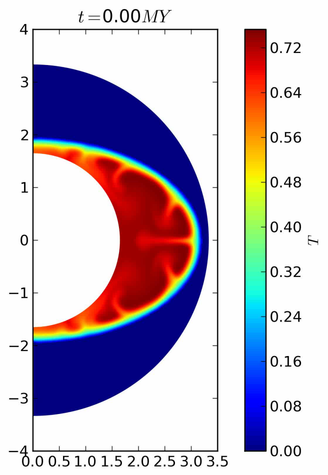

Manual Exponential Despinning

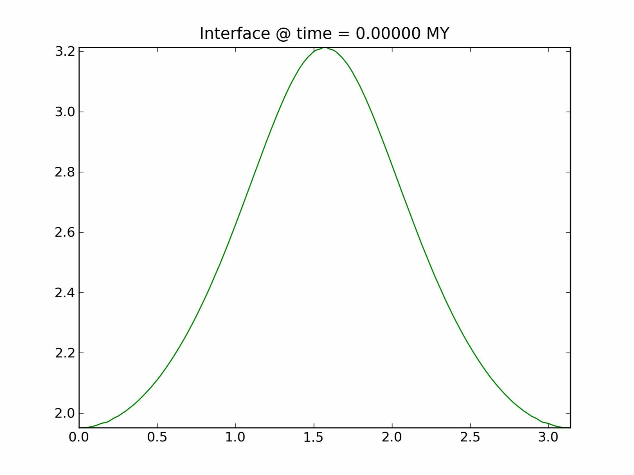

Manual Exponential Despinning

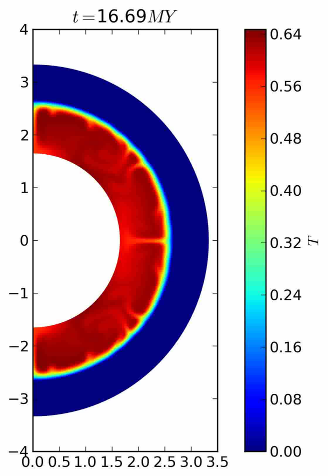

Manual Exponential Despinning

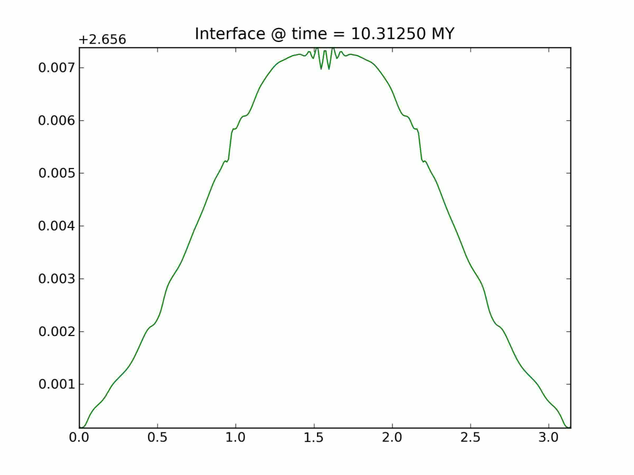

Manual Exponential Despinning

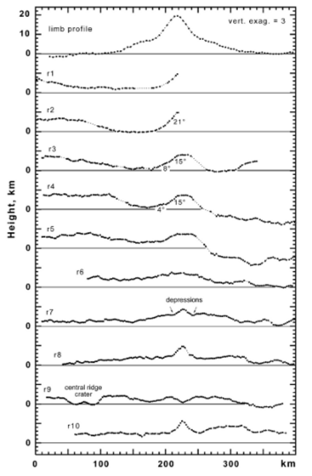

Figure: Iapetian ridge profile Giese et al. [2008]

Manual Exponential Despinning

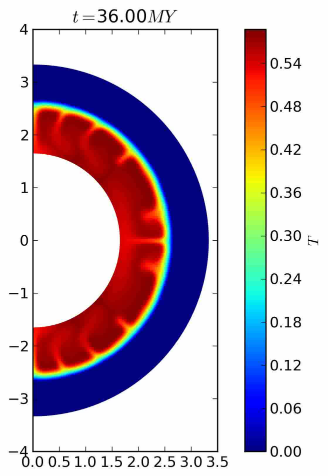

Manual Exponential Despinning

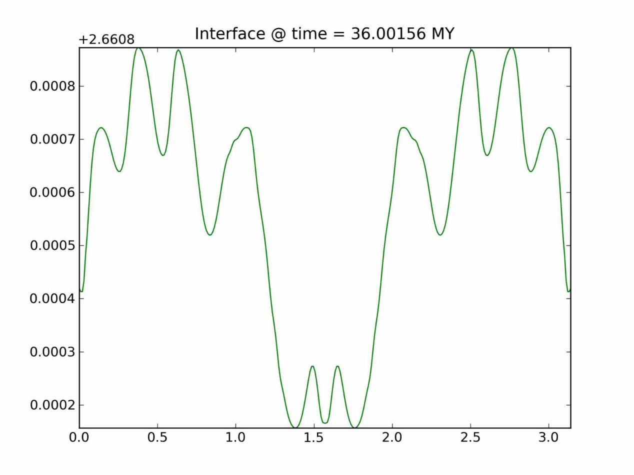

Consistent Despinning

- $E = 50\,\mathsf{kJ.mol}^{-1}$: $\eta_{\mathsf{max}} = 10^{22}\ Pa.s$, $\eta_{\mathsf{air}} = 10^{19}\ Pa.s$

Consistent Despinning

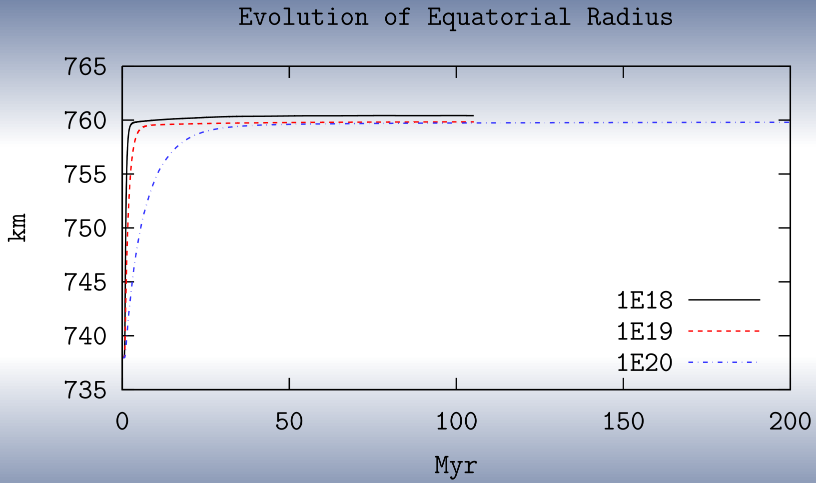

Consistent Despinning

- $E = 50 \times 10^3$ kJ.mol^{-1}: $\eta_{\text{max}} = 10^{22}\, Pa.s$, $\eta_{\text{air}} = 10^{19}\, Pa.s$
- IC: $T(\vec{x}, 0) = T_{\text{int}}$ due to SLRI
- spin-rate evolution:

$$\frac{d\omega}{dt} = \frac{3}{2}\frac{k_2\left(t\right)GM_p^2 a\left(t\right)^5}{D^6 Q\left(t\right)C\left(t\right)}$$

- Andrade rheology:

$$\boldsymbol{\sigma}(t) - \eta \text{sym}(\nabla\vec{v}) = -\int_0^t \frac{\eta}{\mu}\boldsymbol{\sigma}(\tau)\,\mathrm{d}\tau - \int_0^t \alpha\beta(t-\tau)^{\alpha-1}\boldsymbol{\sigma}(\tau)\,\mathrm{d}\tau$$

Aarhenius + Plasticity with Convection

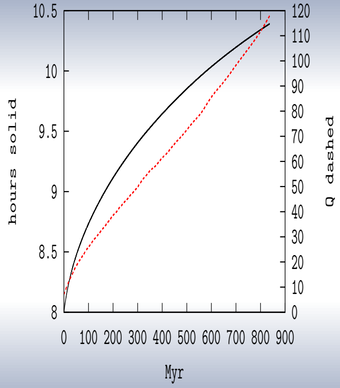

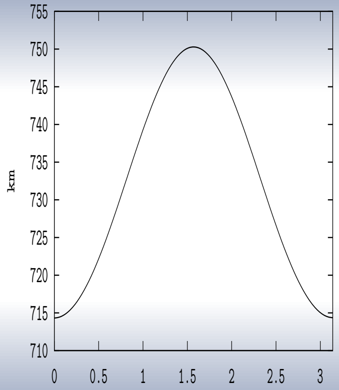

Aarhenius + Plasticity without Convection

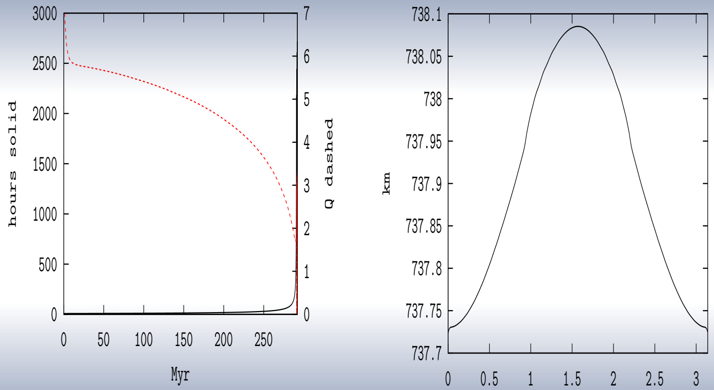

Delayed Convection, $T_{\text{init}} = 240\ K$

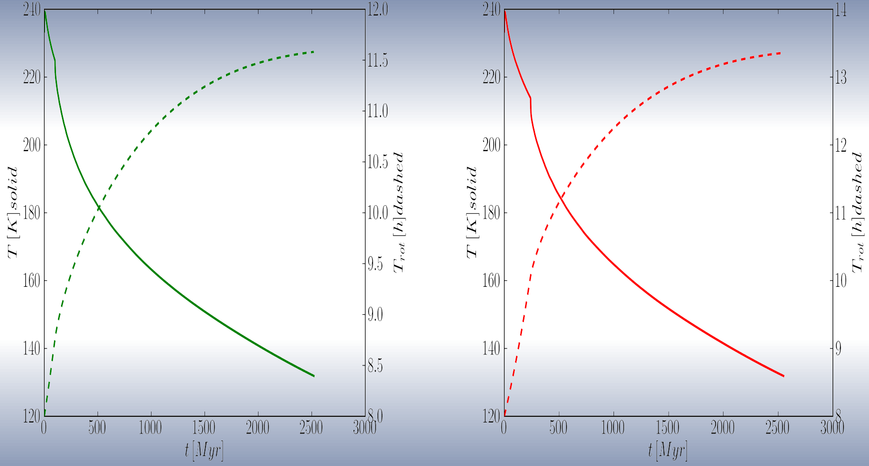

Delayed Convection, $T_{\text{init}} = 240\ K$

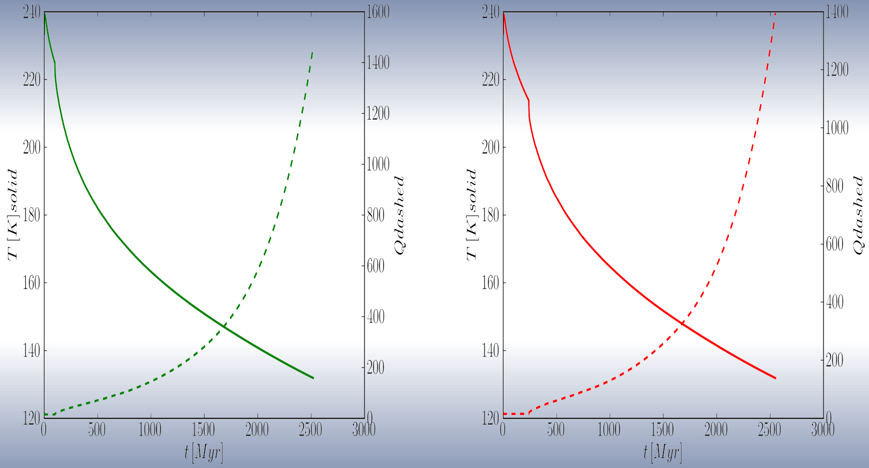

Delayed Convection, $T_{\text{init}} = 240\,K$

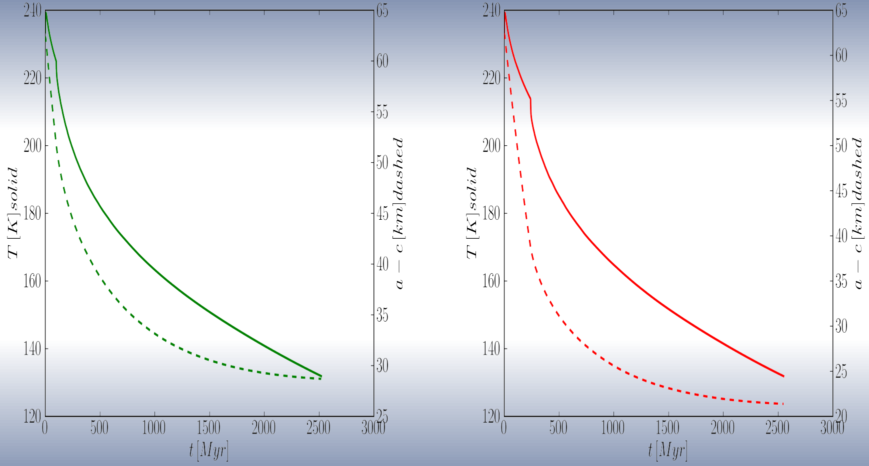

Delayed Convection, $T_{\text{init}} = 260\ K$

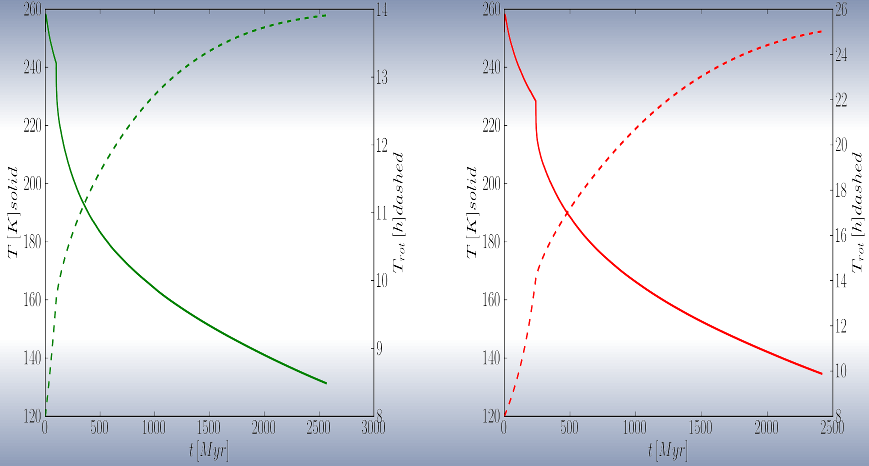

Delayed Convection, $T_{\text{init}} = 260\ K$

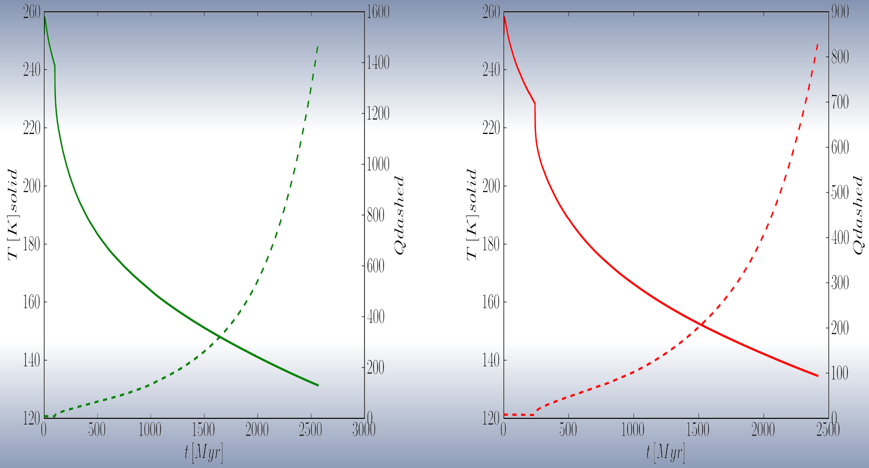

Delayed Convection, $T_{\text{init}} = 260\ K$

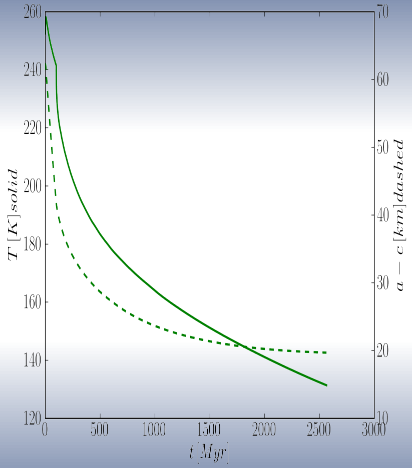

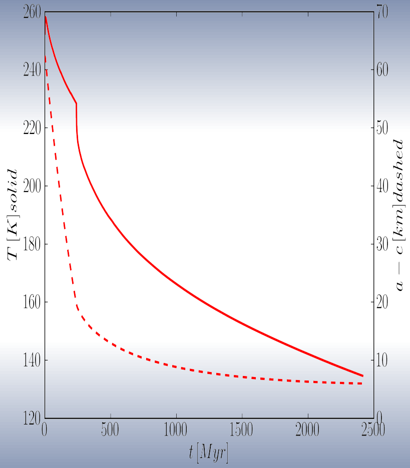

Delayed Convection, $T_{\text{init}} = 270\,K$

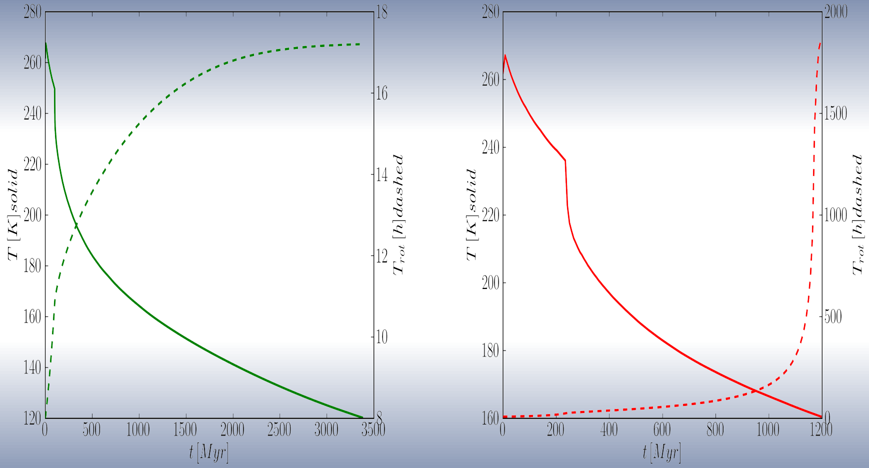

Delayed Convection, $T_{\text{init}} = 270\,K$

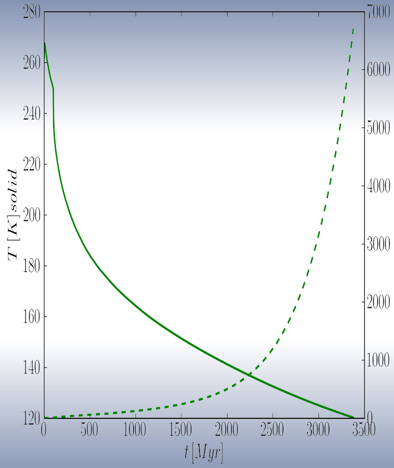

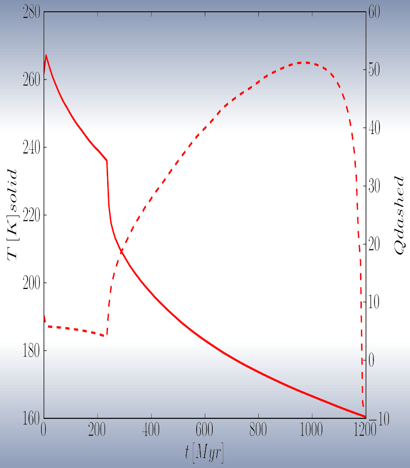

Delayed Convection, $T_{\text{init}} = 270\,K$

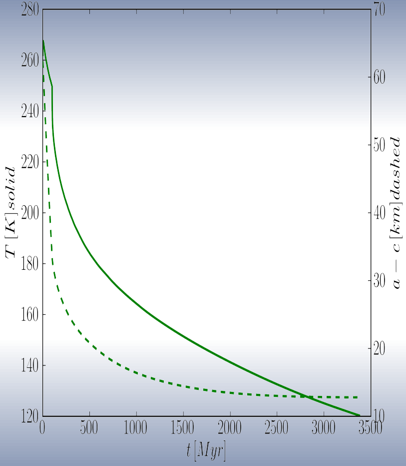

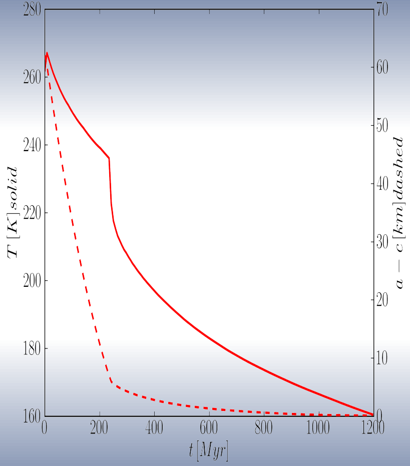

Deformation Mechanisms of Ice

- dislocation creep, superplastic flow, basal slip creep follow

$$\dot{\epsilon} = A\frac{\sigma^n}{d^p}\exp\left(-\frac{Q+PV}{RT}\right)$$

Regime	A $\mathrm{MPa}^{-n}\mathrm{s}^{-1}$	n	Q $\mathrm{kJ.mol}^{-1}$
Dislocation $T < 258$ K	4.0×10^{5}	4	60
Dislocation $T > 258$ K	6.0×10^{28}	4	180
Superplatic $T > 255$ K	3.9×10^{-3}	1.8	49
Superplasic $T > 255$ K	3.0×10^{26}	1.8	192
Basal slip	5.5×10^{7}	2.4	60

Table: Goldsby and Kehlstedt [2001]

- diffusive flow

$$\dot{\epsilon} = \frac{42\sigma V_m}{RTd^2}\left(D_{V,0}\exp\left(-\frac{Q_V}{RT}\right) + \frac{\pi\delta}{d}D_{b,0}\exp\left(-\frac{Q_b}{RT}\right)\right)$$

- constitutive equation

$$\frac{1}{\eta_{TOT}} = \sum_i \frac{1}{\eta_i}$$

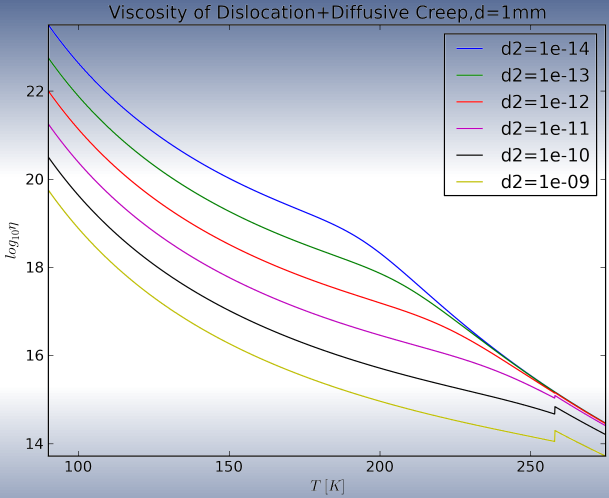
Viscosity of Dislocation+Diffusive Creep,d=1mm
d2=1e-14
d2=1e-13
d2=1e-12
d2=1e-11
d2=1e-10
d2=1e-09
$log_{10}\eta$
22
20
18
16
14
100
150
200
250
$T\,[K]$

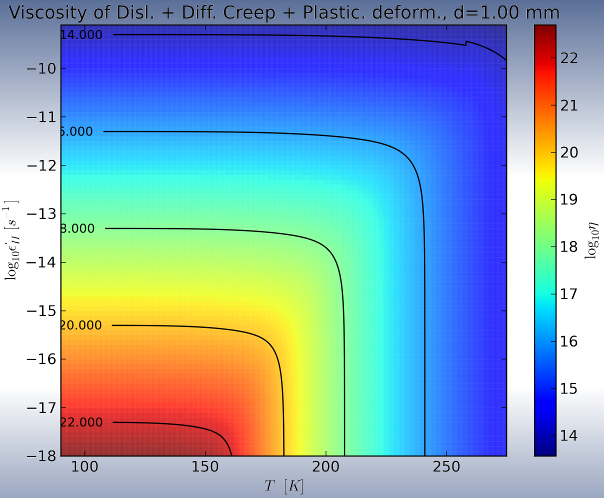
Viscosity of Disl. + Diff. Creep + Plastic. deform., d=1.00 mm
14.000
6.000
8.000
20.000
22.000
−10
−11
−12
−13
−14
−15
−16
−17
−18
100
150
200
250
$T\ [K]$
$\log_{10}\dot{\epsilon}_{II}\ [s^{-1}]$
22
21
20
19
18
17
16
15
14
$\log_{10}\eta$

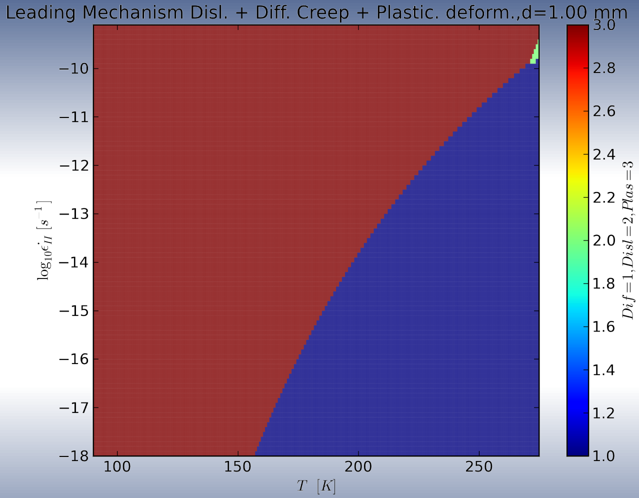
Leading Mechanism Disl. + Diff. Creep + Plastic. deform.,d=1.00 mm
$\log_{10}\dot{\epsilon}_{II}\ [s^{-1}]$
−10
−11
−12
−13
−14
−15
−16
−17
−18
100
150
200
250
$T\ [K]$
3.0
2.8
2.6
2.4
2.2
2.0
1.8
1.6
1.4
1.2
1.0
$Dif=1, Disl=2, Plas=3$

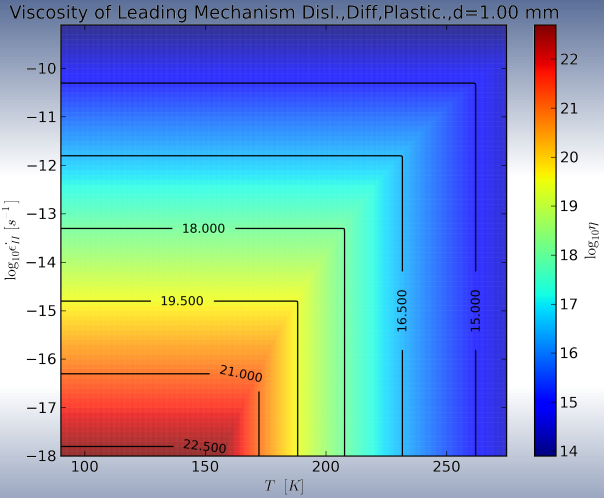
Viscosity of Leading Mechanism Disl.,Diff,Plastic.,d=1.00 mm
$\log_{10}\dot{\epsilon}_{II}\ [s^{-1}]$
−10
−11
−12
−13
−14
−15
−16
−17
−18
100
150
200
250
$T\ [K]$
18.000
19.500
21.000
22.500
16.500
15.000
22
21
20
19
18
17
16
15
14
$\log_{10}\eta$

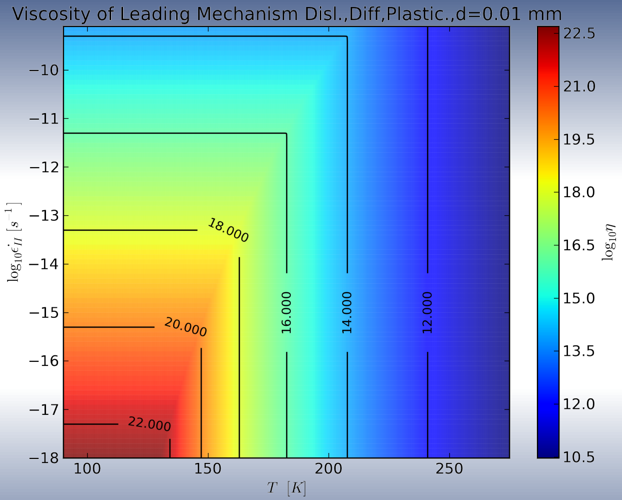
Viscosity of Leading Mechanism Disl.,Diff,Plastic.,d=0.01 mm
$\log_{10}\dot{\epsilon}_{II}\ [s^{-1}]$
−10
−11
−12
−13
−14
−15
−16
−17
−18
100
150
200
250
$T\ [K]$
18.000
20.000
22.000
16.000
14.000
12.000
22.5
21.0
19.5
18.0
16.5
15.0
13.5
12.0
10.5
$\log_{10}\eta$

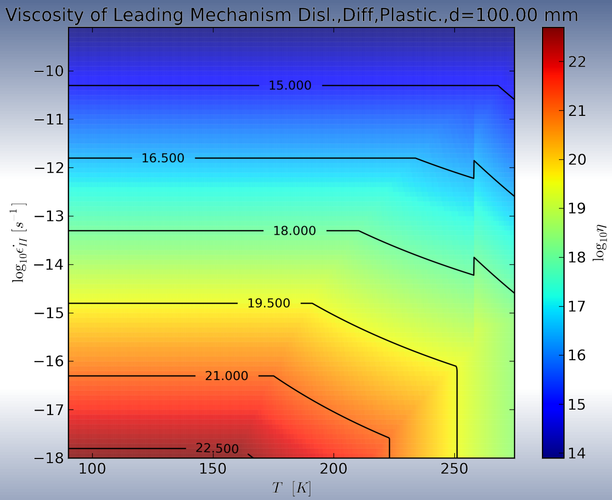
Viscosity of Leading Mechanism Disl.,Diff,Plastic.,d=100.00 mm
15.000
16.500
18.000
19.500
21.000
22.500
−10
−11
−12
−13
−14
−15
−16
−17
−18
$\log_{10}\dot{\epsilon}_{II}\ [s^{-1}]$
100
150
200
250
$T\ [K]$
22
21
20
19
18
17
16
15
14
$\log_{10}\eta$

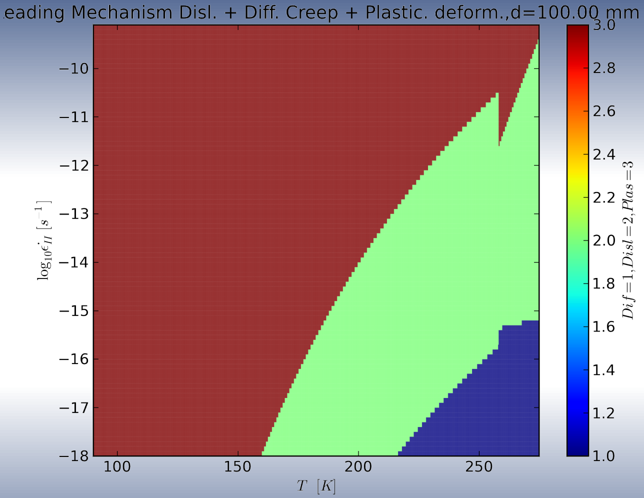

eading Mechanism Disl. + Diff. Creep + Plastic. deform.,d=100.00 mm
$\log_{10}\dot{\epsilon}_{II}\ [s^{-1}]$
−10
−11
−12
−13
−14
−15
−16
−17
−18
100
150
200
250
$T\ [K]$
3.0
2.8
2.6
2.4
2.2
2.0
1.8
1.6
1.4
1.2
1.0
$Dif=1, Disl=2, Plas=3$

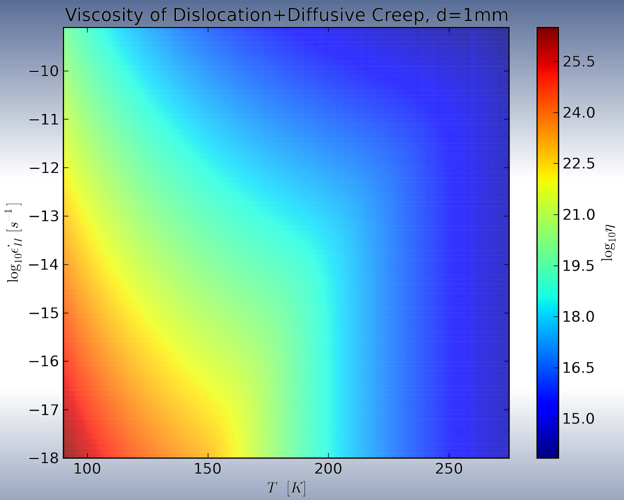
Viscosity of Dislocation+Diffusive Creep, d=1mm
$\log_{10}\dot{\epsilon}_{II}\ [s^{-1}]$
−10
−11
−12
−13
−14
−15
−16
−17
−18
100
150
200
250
$T\ [K]$
25.5
24.0
22.5
21.0
19.5
18.0
16.5
15.0
$\log_{10}\eta$

Diffusive Flow + Dislocation Creep + Plasticity

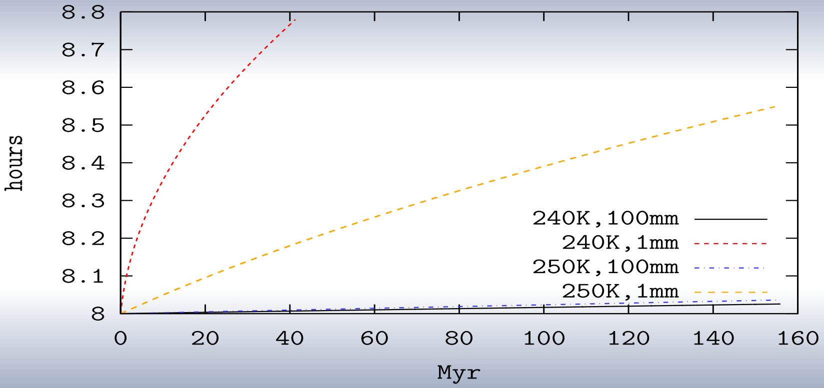

Diffusive Flow + Dislocation Creep + Plasticity

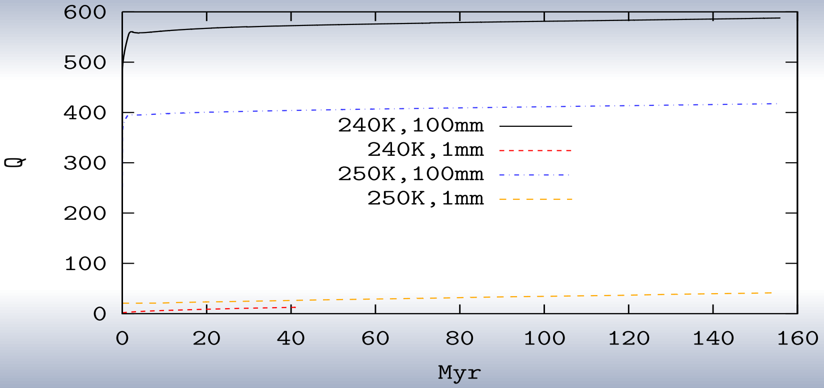

Diffusive Flow + Dislocation Creep + Plasticity

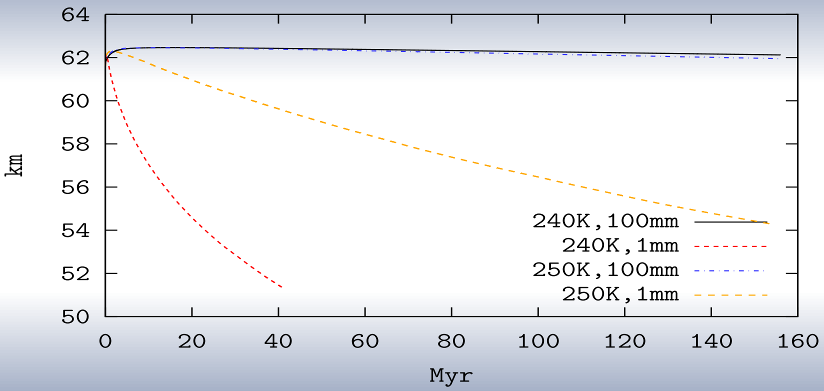

Diffusive Flow + Dislocation Creep + Plasticity

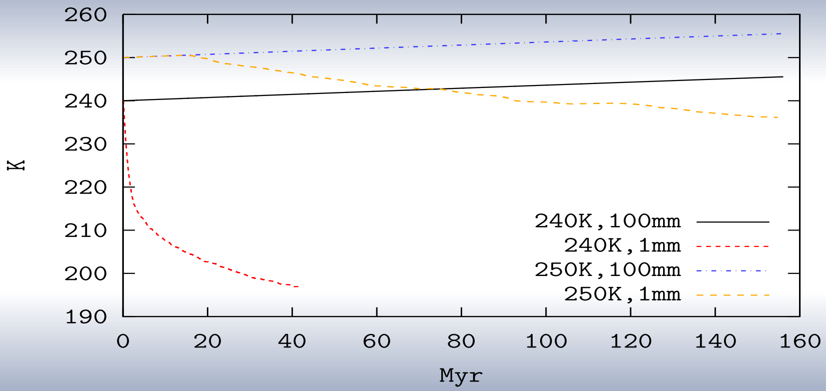

Diffusive Flow + Dislocation Creep + Plasticity

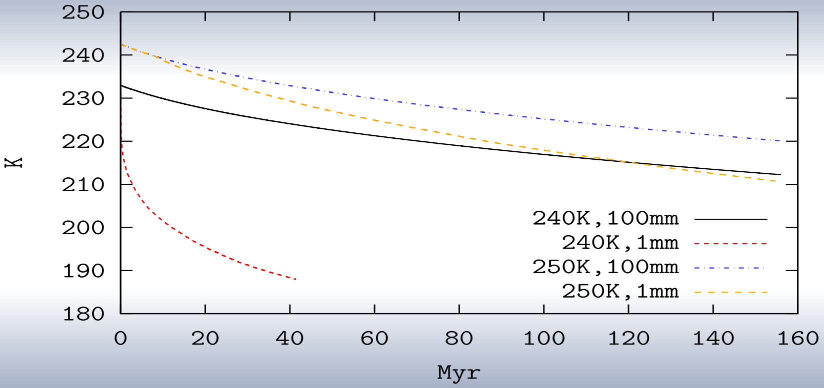

DDP, $d = 1$ mm; $T_{\text{init}} = 240$K

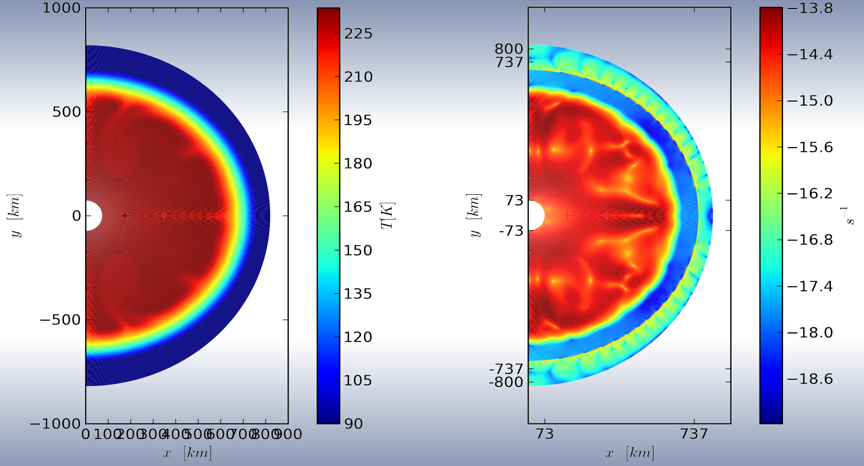

DDP, $d = 1$ mm; $T_{\text{init}} = 240$K

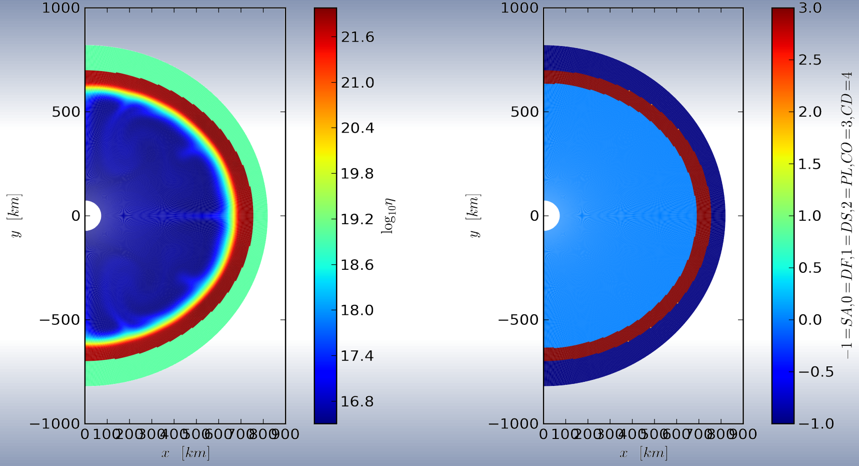

J. C. Castillo-Rogez, D. L. Matson, C. Sotin, T. V. Johnson, J. I. Lunine, and P. C. Thomas. Iapetus' geophysics: Rotation rate, shape, and equatorial ridge. **ICARUS**, 2007.

L. Czechowski and J. Leliwa-Kopystynski. The Iapetus's ridge: Possible explanations of its origin. **ADVANCES IN SPACE RESEARCH**, 2008.

Bernd Giese, Tilmann Denk, Gerhard Neukum, Thomas Roatsch, Paul Helfenstein, Peter C. Thomas, Elizabeth P. Turtle, Alfred McEwen, and Carolyn C. Porco. The topography of Iapetus' leading side. **ICARUS**, 193, 2008.

D. L. Goldsby and D. L. Kehlstedt. Superplastic deformation of ice: Experimental observations. **JOURNAL OF GEOPHYSICAL RESEARCH**, 106, 2001.

W. H. Ip. On a ring origin of the equatorial ridge of Iapetus. **GEOPHYSICAL RESEARCH LETTERS**, 2006.

H. F. Levison, K. J. Walsh, A. C. Barr, and L. Dones. Ridge formation and de-spinning of Iapetus via an impact-generated satellite. **ICARUS**, 2011.

G. Robuchon, G. Choblet, G. Tobie, O. Cadek, C. Sotin, and O. Grasset. Coupling of thermal evolution and despinning of early Iapetus. **ICARUS**, 2010.

David Sandwell and Gerald Schubert. A contraction model for the flattening and equatorial ridge of Iapetus. **ICARUS**, 2010.